The signature C=C=O stretch of propenylketenes and ketene clusters

Khaled El-Shazly, Elizabeth Sparks, Kathryn Narkin, Heather R. Legg, Julia M. Cardot, Matthew A. Hostetler, Laura R. McCunn*

Department of Chemistry, Marshall University
1 John Marshall Dr. Huntington, West Virginia 25755

Carol A. Parish

Department of Chemistry, University of Richmond
Gottwald Center for the Sciences, Richmond, Virginia 23173

A combined experimental and theoretical approach has been used to examine the signature antisymmetric C=C=O stretch of prop-1-enylketene and prop-2-enylketene, as well as a series of ketene multimers and hydrates. Optimization and frequency calculations executed at the B3LYP/6-311G++(d,p) level of theory reveal four conformers of prop-1-enylketene and three conformers of prop-2-enylketene. These ketenes were generated via the pyrolysis of 3-pentenoic anhydride and 4-pentenoic anhydride, respectively, and isolated in low-temperature argon matrices prior to FTIR analysis. The resultant spectra display several bands consistent with B3LYP predictions. A similar computational and experimental survey of ketene multimers and hydrates, generated by the pyrolysis of acetic anhydride, has generated a list of frequencies for the antisymmetric C=C=O stretching mode. The results provide useful benchmarks for identification of propenylketenes in future experiments as well as insight for assigning other substituted ketenes in infrared spectra.

INTRODUCTION

Ketene, $H_2C=C=O$, is an important intermediate in the high-temperature combustion and pyrolysis of hydrocarbons.[1-5] Accordingly, it has been well characterized spectroscopically[6-8] and thoroughly studied for understanding of its reaction mechanisms in high-temperature environments. Substituted ketenes, $R_1R_2C=C=O$, are also important intermediates in pyrolysis and oxidation of hydrocarbons.[9-10] They are especially important to the mechanisms of oxygenated hydrocarbons that are key components of biofuels.[11-13] They also have many applications in organic synthesis,[14] polymers,[15] and catalytic processes.[16] Given the importance of substituted ketenes to many chemical processes, it is important to spectroscopically

characterize these molecules, particularly via infrared absorption, for detection and identification in experiments.

The characteristically strong antisymmetric C=C=O stretch (ν_2) of ketene and its substituted variants is by far the most intense.[6, 8, 17] In one of the earliest comprehensive measurements of the vibrational spectrum of condensed-phase ketene, Moore and Pimentel[8] reported the ν_2 mode at 2142 cm^{-1} in an argon matrix, and 2133 cm^{-1} in the pure solid. A reliable assignment of ketene, and substituted ketenes, would preferably include more than one vibrational band, so it is important to consider other prominent modes. The next strongest mode of ketene in the solid, ν_1, appears at 3043 cm^{-1} (3062 cm^{-1} in the argon matrix). In the argon-matrix spectra, the ν_5 band at 525 cm^{-1} was highest in intensity after ν_2. The relative peak intensities for ν_2 and ν_1 observed by Moore and Pimentel in the solid phase were reported as ∞ and 1.2, respectively. Calculated B3LYP/cc-pVDZ intensities of ketene by Winter *et al.*[18] are 28.5, 564.7, and 25.8 $km \cdot mol^{-1}$ for ν_1, ν_2, and ν_5, respectively. For the well-characterized and simplest substituted analogue methylketene,[18] the strongest mode, ν_4, appears in an argon matrix at 2130 cm^{-1} with a B3LYP-calculated intensity of 619.3 $km \cdot mol^{-1}$ and the next strongest mode, ν_{16}, appears at 551 cm^{-1} with 46.5 $km \cdot mol^{-1}$ calculated intensity. The vast disparity in intensities between the antisymmetric C=C=O stretch and the next most intense band can present an obstacle to confidently assigning a substituted ketene. When experimental conditions preclude the production of large concentration of a substituted ketene, often the antisymmetric C=C=O stretching mode is the only discernable vibrational mode, as the other modes are too comparatively small to rise above the noise.

Gano and Jacob[19] studied the effects of substitution on the antisymmetric C=C=O stretch of ketene. Using argon-matrix FTIR frequencies from the literature and their own experiments

on $X_2C=C=O$, where X = H, CN, Cl, CH_3, and t-butyl, parameters for the Swain-Lupton approach were determined in order to predict the antisymmetric ketene stretching frequency based on an inductive field parameter and a resonance parameter. McAllister and Tidwell[17] furthered efforts to develop accurate prediction methods for the antisymmetric stretch of substituted ketenes by surveying a range of mono- and di-substituted ketenes with *ab initio* molecular orbital calculations at the HF/6-31G* and MP2/6-31G* levels of theory. The calculated frequencies were compared to available argon-matrix FTIR literature values.

Many substituted ketenes have been isolated in low-temperature matrices for FTIR analysis. These include simple alkyl-substituted ketenes like methylketene,[18, 20-21] ethylketene,[11, 22] and dimethylketene,[23] as well as more complex cyclic and conjugated alkylketenes.[24-29] Ketenes incorporating nitrogen-based functional groups such as cyanoketene,[30] imidoylketene[31] and ketenimines[31-32] have been observed. Oxygenated ketenes including hydroxy,[33-34] alkoxy,[30, 35] and carbonyl[36-40] functional group substituents, and also halogenated ketenes including chlorine or bromine atoms[30, 35, 41-43] have also been observed. All of these substituted ketenes have been generated by flash vacuum pyrolysis or photolysis.

Matrix-isolation FTIR spectroscopy is a technique well suited for the detection of molecules that are unstable, including the many substituted ketenes. Matrix-isolation FTIR instruments can easily be coupled to pyrolysis or photolysis sources. The combination of techniques is perfect for generating and characterizing ketenes. It is also very appropriate for an undergraduate research laboratory, in both budget and skill level. Pyrolysis and matrix-isolation FTIR require no high powered lasers or pulsed high voltages that could be dangerous for undergraduate students doing independent laboratory work. The experiments are also is

intellectually accessible to undergraduate chemistry students; even a first-year student can be trained to work independently within a semester.

The purpose of this work is to examine the signature stretching mode of two unsaturated alkylketenes, prop-1-enylketene ($CH_3CH=CHCH=C=O$) and prop-2-enylketene ($CH_2=CHCH_2CH=C=O$), as well as those of ketene multimers and ketene hydrates through a combined approach of matrix-isolation FTIR and *ab initio* calculations. Gas-phase pyrolysis was used to generate the substituted ketenes from appropriate precursor molecules. The results will be instructive in understanding the effect of overall chemical structure on the vibrational modes of ketenes. They will also serve a practical purpose of providing both experimental and computational benchmarks for the identification of a wide range of ketenes in matrix-isolation FTIR experiments, lending insight for the identification in other environments.

METHODS

Pyrolytic Generation and Matrix-Isolation FTIR of Ketenes

Prop-1-enylketene and prop-2-enylketene were generated by gas-phase pyrolysis of 3-pentenoic anhydride (synthesis described below) and 4-pentenoic anhydride (Sigma-Aldrich, 98%), respectively. (Scheme 1) Ketene was generated by pyrolysis of acetic anhydride (Fisher, ≥97%) for the purpose of characterizing ketene multimers and ketene-water complexes. The precursors were degassed and used without further purification. In each case, vapor of the precursor molecule was mixed with 1000 Torr ultra-high purity argon using standard manometric techniques. The concentration of precursor in the mixture ranged from 0.01 to 0.4%, depending on the room-temperature vapor pressure of the precursor as well as the goal of suppressing or promoting multimer/complex formation. The mixture was expanded through a resistively heated silicon carbide (SiC) tube, with a length of 38 mm and inner diameter of 1 mm, mounted on the

face of a pulsed valve (General Valve Series 9).[44] The pyrolysis temperature (800-1200 K) was controlled by a Series 16A temperature controller (Love Controls) and measured by a type C thermocouple mounted on the outside of the SiC tube. The pyrolysis products were isolated in an argon matrix on a 15 K cesium iodide window mounted in a cryostat (Janis Research) with a base pressure of 1.0 x 10^{-6} Torr. The CsI window was cooled by a closed-cycle helium refrigerator (Sumitomo Heavy Industries Ltd.) and its temperature was regulated by a Lake Shore 331 Temperature Controller. Prior to recording an FTIR spectrum, the window was cooled to 4 K. FTIR spectra were collected for 128 scans at 0.5 cm^{-1} resolution with a Bruker Vertex 70 spectrometer that was purged with dry air. The apparatus for pyrolysis and matrix-isolation FTIR has been described in detail previously.[45] Optimization and frequency calculations were performed on all substituted ketenes and ketene complexes at the B3LYP/6-311G++(d,p) level of theory using Gaussian 09.[46]

Synthesis of 3-Pentenoic Anhydride

To a solution of 3-pentenoic acid (2.02 mL, 20.0 mmol) in CH_2Cl_2, (50 mL) was added *N,N'*-diisopropylcarbodiimide (1.55 mL, 9.99 mmol) dropwise at room temperature. The resulting solution was allowed to stir at room temperature for 1.5 hours, at which point the reaction was determined to be complete by thin layer chromatography. The reaction was quenched with saturated aqueous $NaHCO_3$, and the organic layer was washed with saturated aqueous NaCl. The organic layer was dried over Na_2SO_4, filtered, and concentrated under reduced pressure. The resulting crude residue was purified by flash column chromatography (10% EtOAc/hexane) to afford 3-pentenoic anhydride (725 mg, 40%) as a colorless oil: ^{1}H NMR (400 MHz, $CDCl_3$): δ 5.69 – 5.46 (m, 4H), 3.18 – 3.15 (m, 4H), 1.73 – 1.70 (m, 6H). ^{13}C NMR (100 MHz, $CDCl_3$): δ 168.0, 131.3, 121.0, 39.0, 18.2.

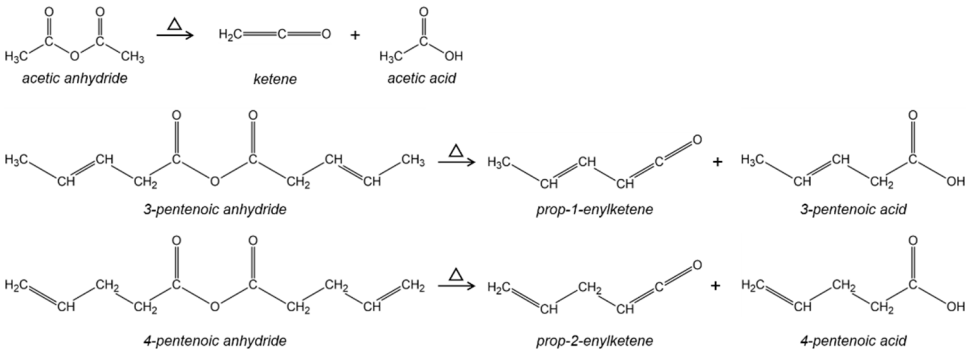

Scheme 1. Pyrolytic generation of ketene and propenylketenes

RESULTS AND DISCUSSION

A) Ketene multimers and hydrates

The pyrolysis of acetic anhydride was employed to generate ketene and to determine the optimal conditions for isolating ketene while avoiding ketene multimers and ketene-water complexes that could complicate the spectrum and interfere with the assignment of substituted ketenes in other pyrolysis experiments. Figure 1 shows the matrix-isolation FTIR spectra collected following pyrolysis of acetic anhydride at different temperatures and concentrations in argon. The spectrum collected following 800 K pyrolysis of 0.01% acetic anhydride provides satisfactory absorbance for the antisymmetric stretch at 2142 cm^{-1} while minimizing the contributions from ketene complexes observed at 2125-2138 cm^{-1}. Other characteristic bands[8, 47] of ketene were observed at 3155, 3063, 1380, 1114, 973, 590, and 524 cm^{-1}.

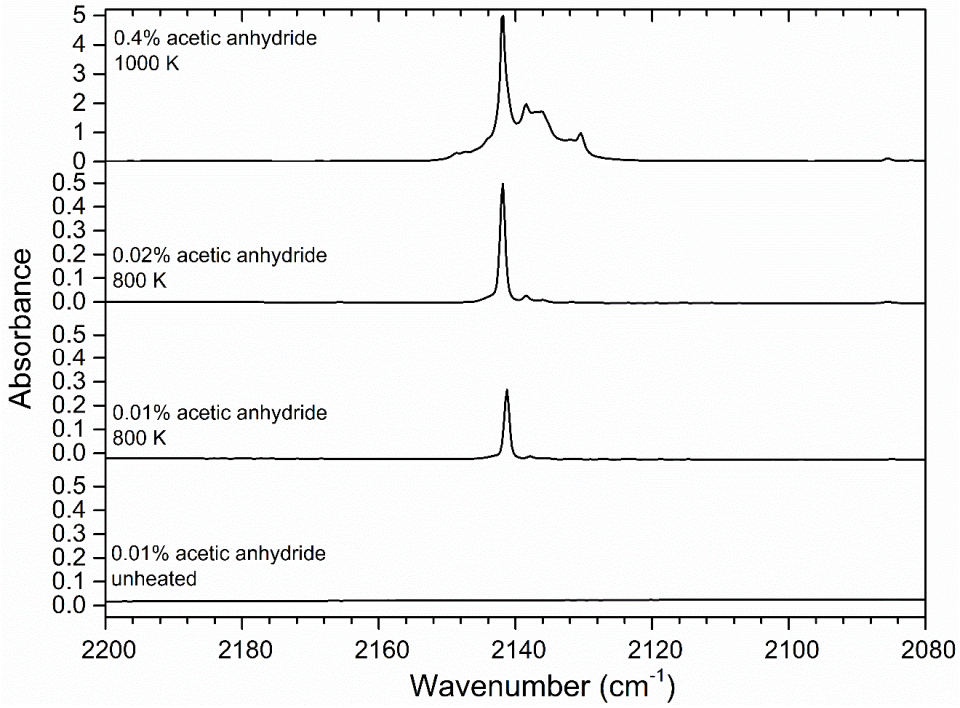

Figure 1. Matrix-isolation FTIR spectra (4 K) recorded following the pyrolysis at 800 K and 1000 K of acetic anhydride in argon. The bottom trace shows the spectrum of an unheated sample as a control.

The top trace in Figure 1 shows significant contributions from many ketene complexes in the 2125-2138 region, a result of the high concentration of acetic anhydride. The most prominent bands at 2138, 2136, and 2130 cm^{-1} are presumed to belong to ketene multimers or ketene-water complexes. To facilitate the assignment, electronic structure calculations were undertaken on ketene dimers, trimers, and tetramers, as well as complexes of ketene with one or two water molecules. Table 1 shows the experimental and computationally predicted frequencies used to obtain a proper scaling factor for the calculated C=C=O antisymmetric stretching frequencies that could then be applied to calculated frequencies of the ketene multimers and hydrates, as well as those of substituted ketenes like prop-1-enylketene and prop-2-enylketene isolated in a 4 K argon matrix. Table 2 shows the calculated ν_2 bands, raw and scaled, as well as intensities for the selected ketene multimers and hydrates, with the optimized

structures shown in Figure 2. The ketene·H_2O structures are in agreement with those found by Louie *et al*.[48], although Structure C could not be optimized at the B3LYP/6-311G++(d,p) level of theory so the 6-311G++(3df,3pd) basis set was used instead. The scaled vibrational bands for all of the ketene complexes occur over the range of frequencies observed in the experimental spectrum, 2125-2138 cm^{-1}. Given the overlapping bands in the experimental spectrum, and the closely spaced predicted bands, it is impossible to definitively assign any of the ketene complexes in the spectrum. Nevertheless, it would be reasonable to assume that the most populous clusters in the matrix would be the ketene dimer and ketene·H_2O. The results in Table 2 suggest that these clusters could account for bands at the high end of the 2125-2138 cm^{-1} range. The ketene·$(H_2O)_2$ is more likely to appear at the low end of the range, as well as the ketene tetramer, although that cluster seems less likely to form.

Table 1. Experimental (4 K argon matrix) and computational bands of assorted ketenes and the resultant scaling factor for the C=C=O antisymmetric stretching frequency.

	Experimental frequency (cm^{-1})	Ref.	Raw B3LYP//6-311G++(d,p) frequency (cm^{-1})	Scaling Factor
ketene	2142	[47]	2221	0.9643
methylketene	2126	[49]	2207	0.9632
ethylketene (anticlinal)	2130	[22, 45]	2202	0.9671
ethylketene (synperiplanar)			2201	0.9678
			Average Scaling Factor:	0.9656

Table 2. Antisymmetric stretching frequency (ν_2) in several ketene multimers and ketene hydrates calculated at the B3LYP//6-311G++(d,p) level of theory with predicted intensities ($km \cdot mol^{-1}$) in parentheses.

	Raw B3LYP//6-311G++(d,p) frequency (cm^{-1})	**Scaled[a] ν_2 (cm^{-1})**
ketene dimer (structure A)	2214.7659 (0) 2219.6314 (1353)	2139 2143
ketene dimer (structure B)	2212.7059 (966) 2222.7411 (533)	2137 2146
ketene trimer (structure A)	2207.9594 (0.1) 2217.4268 (1071) 2217.7518 (1071)	2132 2141 2142
ketene trimer (structure B)	2207.9407 (1065) 2217.8971 (818) 2222.6627 (427)	2132 2142 2146
ketene tetramer (structure A)	2199.6528 (0) 2213.7475 (1280) 2213.7477 (1280) 2221.5405 (382)	2130 2138 2144 2146
ketene tetramer (structure B)	2205.3594 (1520) 2213.8038 (521) 2219.8663 (946) 2222.3794 (190)	2130 2138 2144 2146
ketene·H_2O (structure A)	2214.6792 (779)	2139
ketene·H_2O (structure B)	2213.8751 (687)	2138
ketene·H_2O (structure C)	2211.6195 (663)	2136
ketene·$(H_2O)_2$ (structure A)	2203.6034 (714)	2128
ketene·$(H_2O)_2$ (structure B)	2205.1242 (676)	2129

[a]Scaling factor = 0.9656

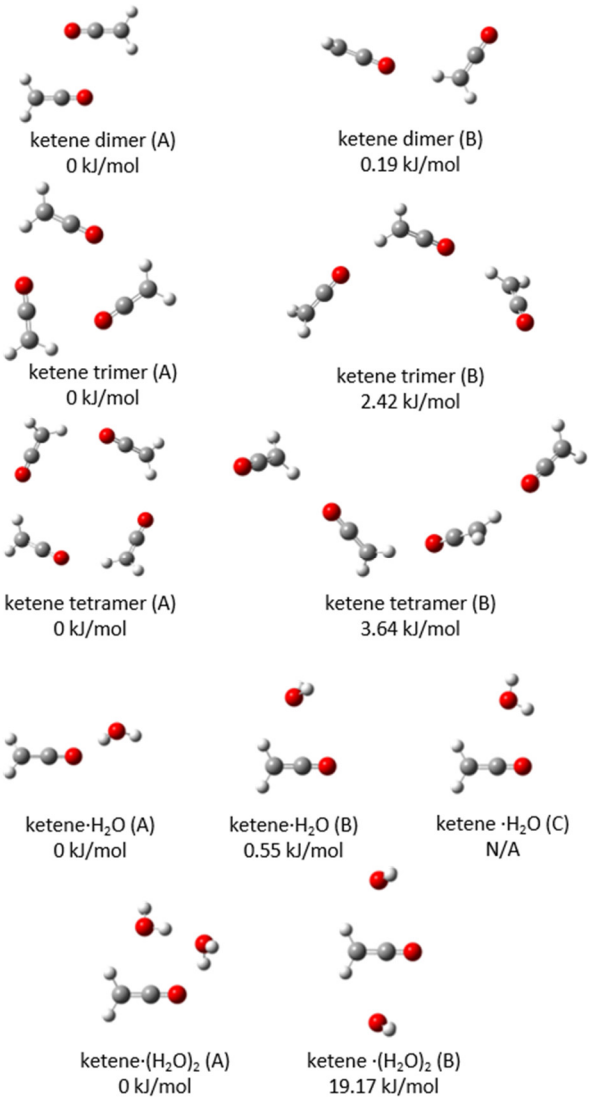

Figure 2. B3LYP-optimized structures for selected ketene multimers and hydrates. Among groups of structures for a given complex, relative energies (kJ/mol) are given under each structure.

B) Prop-2-enylketene

The pyrolysis of 4-pentenoic anhydride generated prop-2-enylketene. Figure 3 shows bands at 2123, 2128, and 2132 cm^{-1}. The bands at 2139 and 2142 cm^{-1} that appear in all three traces are due to CO and ketene, respectively, and are trace contaminants from the pyrolysis source that could be observed even when heating pure argon in the source. The CO and ketene

may also be due to alternate pyrolysis pathways of the anhydride, especially at higher temperatures. Table 3 shows the scaled calculated frequencies for the conformers of prop-2-enylketene. There are three stable conformers of prop-2-enylketene, each defined by two C-C-C-C dihedral angles. (Figure 4) The scaled calculated frequencies are in reasonable agreement with the experimentally observed bands; however, assigning individual conformers to the experimentally observed bands would be speculative because of the close spacing of both the calculated and experimental frequencies, combined with an expected error a few wavenumbers in the scaled frequencies. Prop-2-enylketene is not as stable as ketene under these pyrolysis conditions. The top two traces in Figure 3 show that the bands disappear for pyrolysis at 1000 K and 1200 K, while bands for CO, ketene, and $CO \cdot H_2O$ emerge. This observation highlights the importance of choosing the appropriate temperature for the pyrolytic generation of substituted ketenes in general. A survey of the concentration dependence of the pyrolysis experiments in Figure 5 confirms that the observed bands are not due to any multimers or hydrates of prop-2-enylketene, nor due to any complexes of regular ketene. The bands at 2123, 2128, and 2132 cm^{-1} persist at the lowest concentration of 4-pentenoic anhydride, whereas any cluster peaks should be suppressed in comparison.

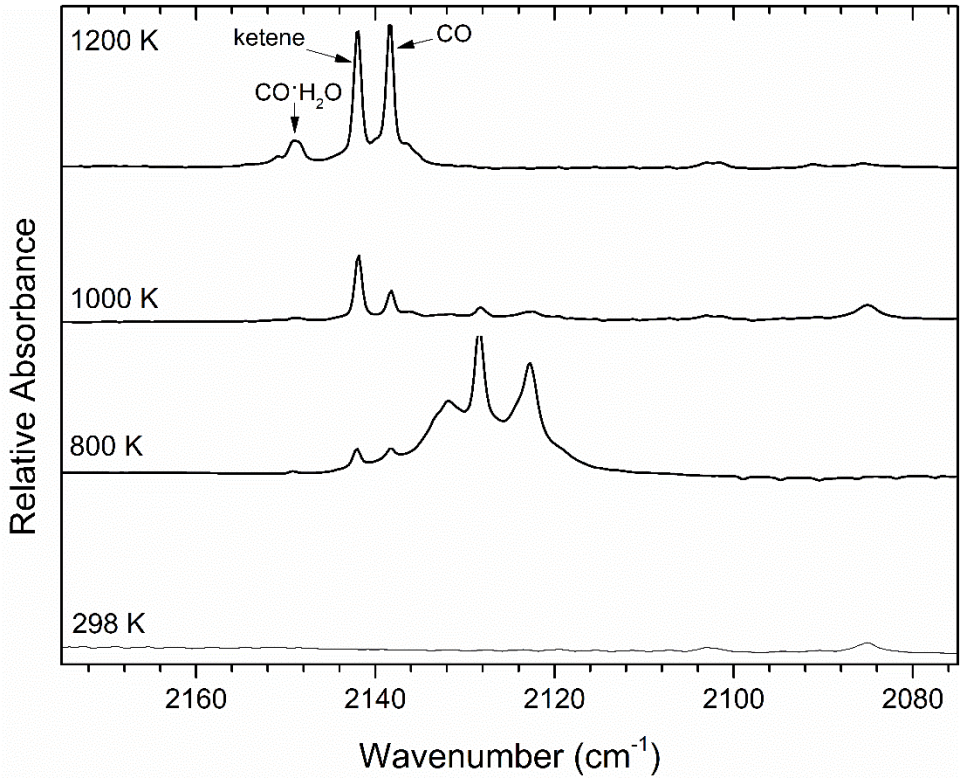

Figure 3. Matrix-isolation FTIR spectra (4 K) recorded following the pyrolysis at 800-1200 K of 4-pentenoic anhydride in argon (0.4% mixtures for all temperatures, except 0.22% for 800 K). The bottom trace shows the spectrum of an unheated sample as a control. The y-axis for each trace has the same magnitude of scale.

Table 3. Antisymmetric stretching frequency in propenylketene conformers calculated at the B3LYP//6-311G++(d,p) level of theory.

	Raw B3LYP//6-311G++(d,p) frequency (cm^{-1})	**Scaled[a] ν_2 (cm^{-1})**
prop-2-enylketene (Conformer A)	2204	2128
prop-2-enylketene (Conformer B)	2207	2132
prop-2-enylketene (Conformer C)	2204	2128
prop-1-enylketene (Conformer A)	2200	2125
prop-1-enylketene (Conformer B)	2201	2125
prop-1-enylketene (Conformer C)	2195	2120
prop-1-enylketene (Conformer D)	2191	2116

[a]Scaling factor = 0.9656

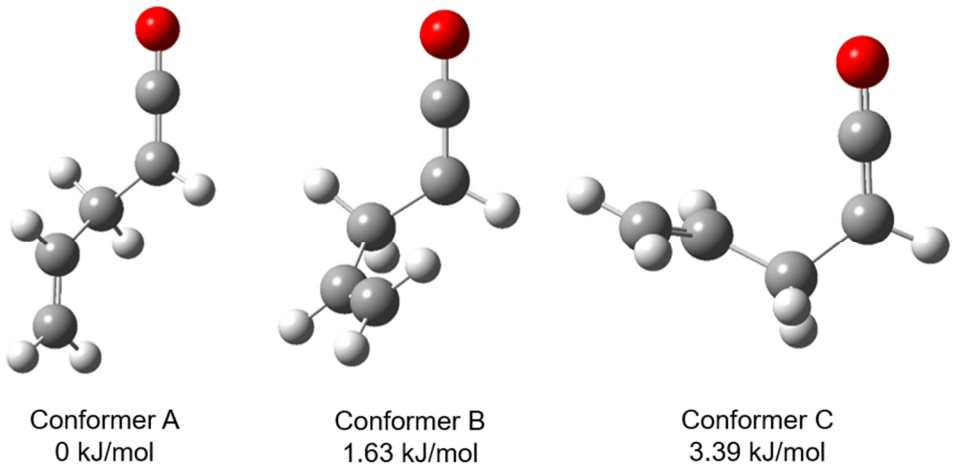

Figure 4. B3LYP/6-311G++(d,p) optimized structures of prop-2-enylketene conformers and relative (zero-point corrected) energies.

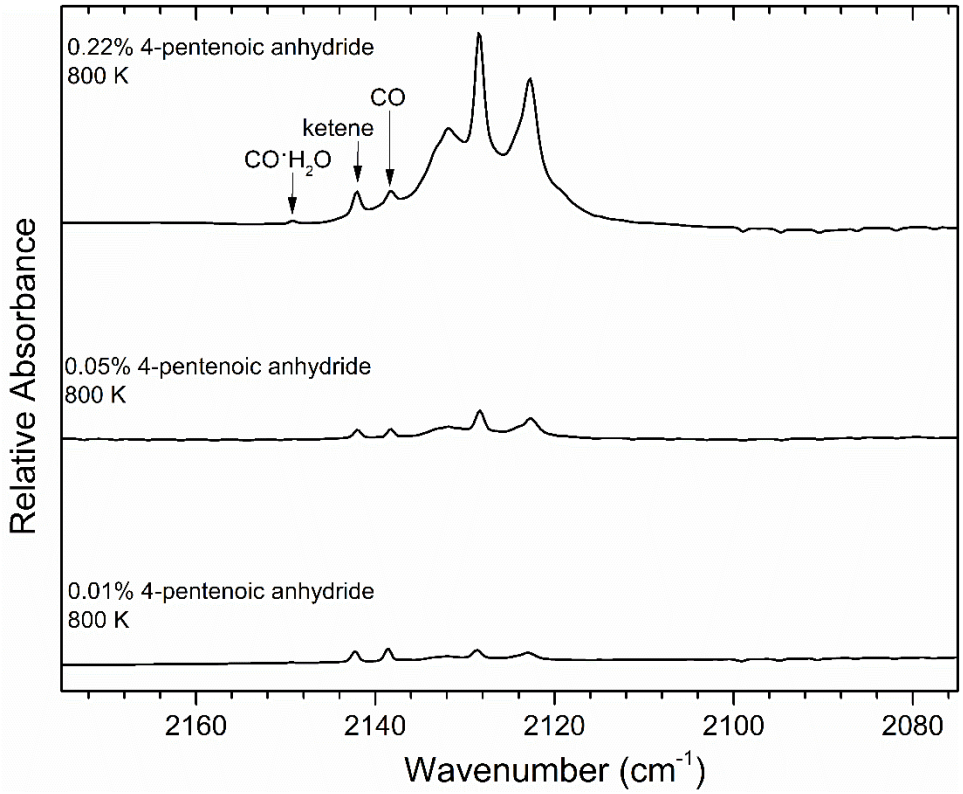

Figure 5. Matrix-isolation FTIR spectra (4 K) recorded following the 800 K pyrolysis of 4-pentenoic anhydride in argon at various concentrations. The y-axis for each trace has the same magnitude of scale.

C) Prop-1-enylketene

The pyrolysis of 3-pentenoic anhydride generated prop-1-enylketene. Figure 6 shows bands at 2128, 2124 and 2115 cm^{-1}. Table 3 shows the scaled calculated frequencies for the four conformers of prop-1-enylketene, each defined by the two C-C-C-C dihedral angles. Optimized structures and relative energies for these conformers are shown in Figure 7. There is satisfactory agreement between the experimental and calculated bands, although assignment of specific conformers is not recommended due to the close spacing of the vibrational bands. The generation of prop-1-enylketene is also sensitive to pyrolysis temperature, but has a different optimal temperature than prop-2-enylketene. Figure 6 shows no signal following pyrolysis at 800 K, but clear features of prop-1-enylketene at 1000 K. At 1200 K, the prop-1-enylketene has undergone subsequent thermal decomposition and been replaced by CO $CO{\cdot}H_2O$ and ketene in the spectrum.

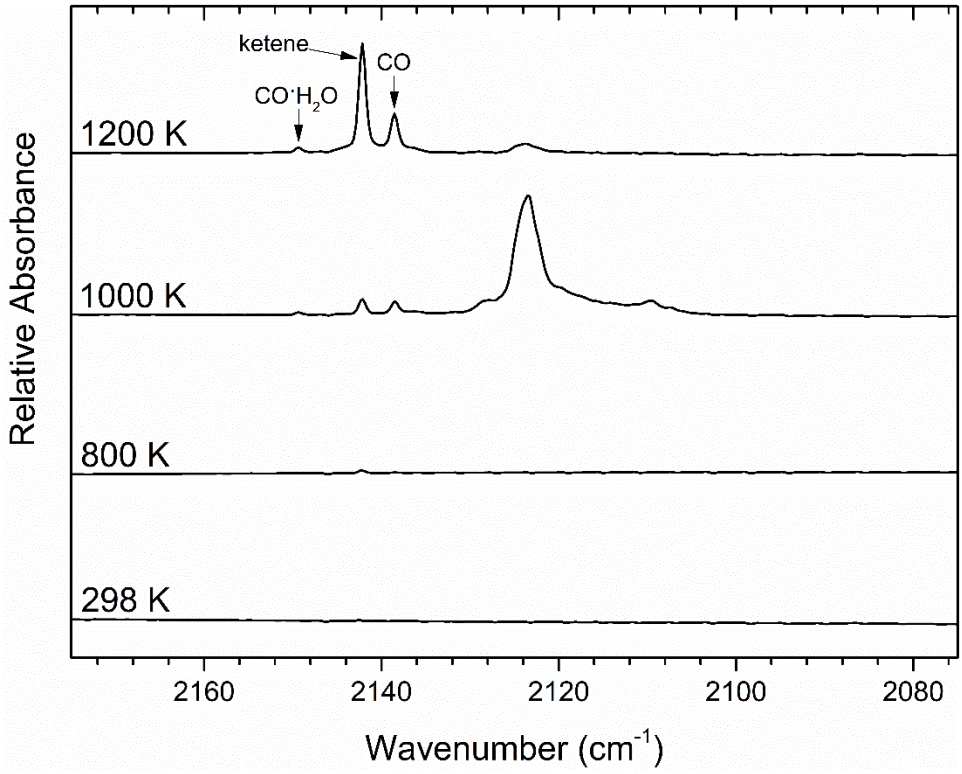

Figure 6. Matrix-isolation FTIR spectra recorded following the pyrolysis of 0.08% 3-pentenoic anhydride in argon at 800-1200 K. The bottom trace shows the spectrum of an unheated sample as a control. The y-axis for each trace has the same magnitude of scale.

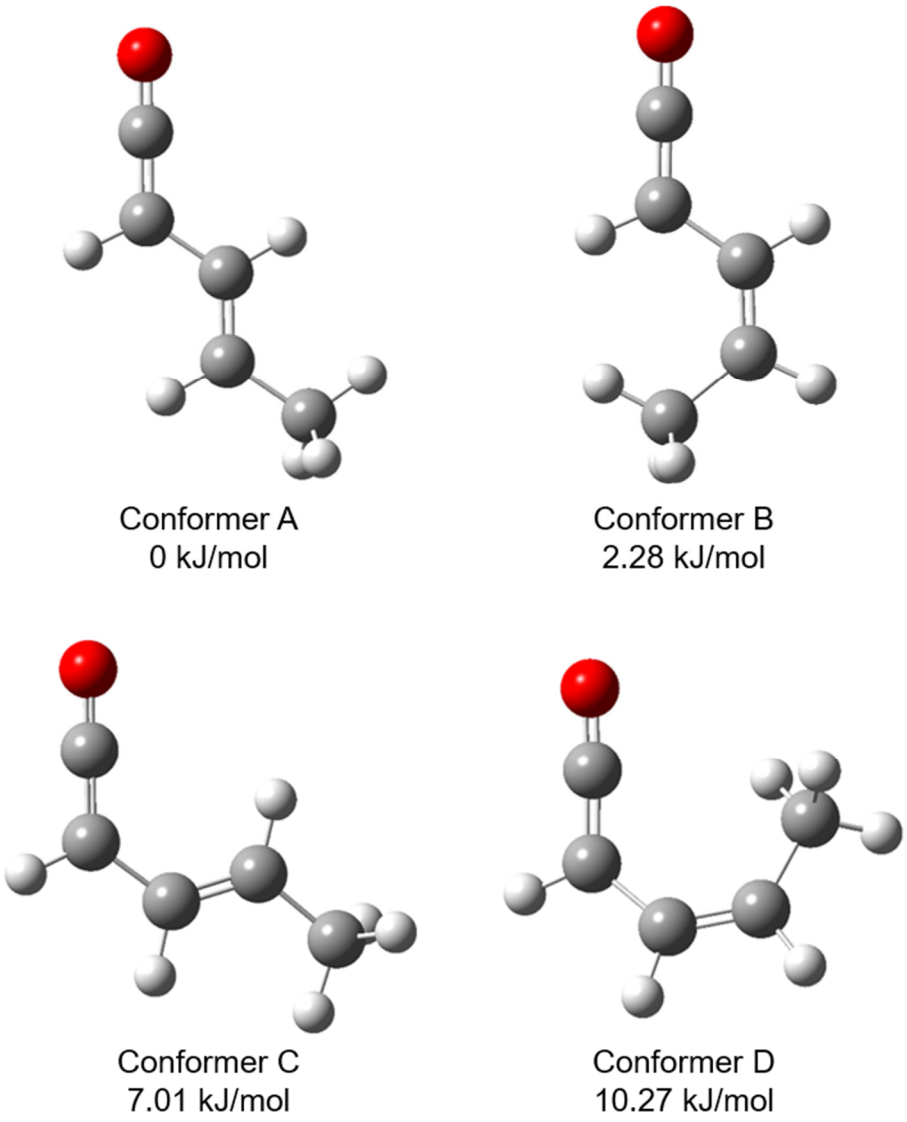

Figure 7. B3LYP/6-311G++(d,p) optimized structures of prop-1-enylketene conformers and relative (zero-point corrected) energies.

CONCLUSIONS

The C=C=O antisymmetric stretching region has been investigated for ketene, several of its complexes, and the propenylketenes. The experimentally observed matrix-isolation FTIR spectra provide useful benchmarks for identification of these species in future experiments. A scaling factor to be applied to B3LYP/6-311G++(d,p) predicted frequencies for the C=C=O

antisymmetric stretch in substituted ketenes will be useful for identification of other species in experiments utilizing matrix-isolation FTIR detection.

ACKNOWLEDGMENTS

This material is based upon work supported by the U.S. Department of Energy, Office of Science under Award Number DE-SC0019732. The authors acknowledge Barney Ellison for helpful insight in the pyrolytic generation of ketenes. HRL acknowledges a William C. Dudley Summer Undergraduate Research Fellowship and the Lacy Stone Memorial Chemistry Scholarship. JMC acknowledges support for research performed during the summer of 2021 from the WV Higher Education Policy Commission, Division of Science and Research under award dsr.20.16. LRM and MAH acknowledge Marshall University Summer Research Awards.

REFERENCES

1. Barnard, J. A.; Kirschner, E. The Slow Combustion of Ketene. *Combust. Flame* **1967,** *11*, 496-500.

2. Christensen, M.; Konnov, A. A. Laminar Burning Velocity of Diacetyl + air Flames. Further Assessment of Combustion Chemistry of Ketene. *Combust. Flame* **2017,** *178*, 97-110.

3. Minwegen, H.; Döntgen, M.; Fenard, Y.; Morsch, P.; Heufer, K. A. Proceeding on the Riddles of Ketene Pyrolysis by Applying Ab Initio Quantum Chemical Computational Methods in a Detailed Kinetic Modeling Study. *Proceedings of the Combustion Institute* **2021,** *38*, 749-755.

4. Sun, W.; Wang, J.; Huang, C.; Hansen, N.; Yang, B. Providing Effective Constraints for Developing Ketene Combustion Mechanisms: A Detailed Kinetic Investigation of Diacetyl Flames. *Combust. Flame* **2019,** *205*, 11-21.

5. Pichon, S.; Black, G.; Chaumeix, N.; Yahyaoui, M.; Simmie, J. M.; Curran, H. J.; Donohue, R. The Combustion Chemistry of a Fuel Tracer: Measured Flame Speeds and Ignition Delays and a Detailed Chemical Kinetic Model for the Oxidation of Acetone. *Combust. Flame* **2009,** *156*, 494-504.

6. Butler, P. E. B.; Eatcw, D. R.; Thompson, H. W. Vibration-Rotation Bands of Keten. *Spectrochimica Acta* **1958,** *13*, 223-235.

7. Arendale, W. F.; Fletcher, W. H. Some Vibration-Rotation Bands of Ketene. *J. Chem. Phys.* **1956,** *24*, 581-587.

8. Moore, C. B.; Pimentel, G. C. Infrared Spectrum and Vibrational Potential Function of Ketene and the Deuterated Ketenes. *J. Chem. Phys.* **1963,** *38*, 2816-2829.

9. Hemberger, P.; Bodi, A.; Bierkandt, T.; Köhler, M.; Kaczmarek, D.; Kasper, T. Photoelectron Photoion Coincidence Spectroscopy Provides Mechanistic Insights in Fuel Synthesis and Conversion. *Energy Fuels* **2021,** *35*, 16265-16302.

10. Sumathi, R.; Green, W. H. Thermodynamic Properties of Ketenes: Group Additivity Values from Quantum Chemical Calculations. *J. Phys. Chem. A* **2002,** *106*, 7937-7949.

11. Porterfield, J. P.; Bross, D. H.; Ruscic, B.; Thorpe, J. H.; Nguyen, T. L.; Baraban, J. H.; Stanton, J. F.; Daily, J. W.; Ellison, G. B. Thermal Decomposition of Potential Ester Biofuels. Part I: Methyl Acetate and Methyl Butanoate. *J. Phys. Chem. A* **2017,** *121*, 4658-4677.

12. Kulyk, K.; Palianytsia, B.; Alexander, J. D.; Azizova, L.; Borysenko, M.; Kartel, M.; Larsson, M.; Kulik, T. Kinetics of Valeric Acid Ketonization and Ketenization in Catalytic Pyrolysis on Nanosized SiO_2, γ-Al_2O_3, CeO_2/SiO_2, Al_2O_3/SiO_2 and TiO_2/SiO_2. *ChemPhysChem* **2017,** *18*, 1943-1955.

13. Wei, L.; Li, Z.; Tong, L.; Wang, Z.; Jin, H.; Yao, M.; Zheng, Z.; Wang, C.; Xu, H. Primary Combustion Intermediates in Lean and Rich Low-Pressure Premixed Laminar 2-Methylfuran/Oxygen/Argon Flames. *Energy Fuels* **2012,** *26*, 6651-6660.

14. Allen, A. D.; Tidwell, T. T. New Directions in Ketene Chemistry: The Land of Opportunity. *Eur. J. Org. Chem.* **2012,** *2012*, 1081-1096.

15. Leibfarth, F. A.; Hawker, C. J. The Emerging Utility of Ketenes in Polymer Chemistry. *Journal of Polymer Science Part A: Polymer Chemistry* **2013,** *51*, 3769-3782.

16. Chowdhury, A. D.; Gascon, J. The Curious Case of Ketene in Zeolite Chemistry and Catalysis. *Angewandte Chemie International Edition* **2018,** *57*, 14982-14985.

17. McAllister, M. A.; Tidwell, T. T. Structural and Substituent Effects on the Ketene Infrared Stretching Frequency. *Can. J. Chem.* **1994,** *72*, 882-887.

18. Winter, P. R.; Rowland, B.; Hess, W. P.; Radziszewski, J. G.; Nimlos, M. R.; Ellison, G. B. UV Photodissociation of Matrix-Isolated Propionyl Chloride. *J. Phys. Chem. A* **1998,** *102*, 3238-3248.

19. Gano, J. E.; Jacob, E. J. Substituent Effects on the Ketene Asymmetric Stretching Frequency. *Spectrochimica Acta Part A: Molecular Spectroscopy* **1987,** *43*, 1023-1025.

20. Harrison, J. A.; Frei, H. Visible Light-Induced Oxygen Transfer from Nitrogen Dioxide to Ethyne and Propyne in a Cryogenic Matrix. 1. Identification of Products. *J. Phys. Chem.* **1994,** *98*, 12142-12151.

21. Dugarte, N. Y.; Erben, M. F.; Romano, R. M.; Boese, R.; Ge, M.-F.; Li, Y.; Della Védova, C. O. Matrix Photochemistry, Photoelectron Spectroscopy, Solid-Phase Structure, and Ring Strain Energy of β-Propiothiolactone. *J. Phys. Chem. A* **2009,** *113*, 3662-3672.

22. Dugarte, N. Y.; Erben, M. F.; Romano, R. M.; Ge, M.-F.; Li, Y.; Della Védova, C. O. Matrix Photochemistry at Low Temperatures and Spectroscopic Properties of γ-Butyrothiolactone. *J. Phys. Chem. A* **2010,** *114*, 9462-9470.

23. Parker, J. K.; Davis, S. R. Photochemical Reaction of Ozone and Dimethylacetylene: An Infrared Matrix Isolation and Ab Initio Investigation. *J. Phys. Chem. A* **1999,** *103*, 7280-7286.

24. Sato, T.; Niino, H.; Yabe, A. Consecutive Photolyses of Naphthalenedicarboxylic Anhydrides in Low Temperature Matrixes: Experimental and Computational Studies on Naphthynes and Benzocyclopentadienylideneketenes. *J. Phys. Chem. A* **2001,** *105*, 7790-7798.

25. Radziszewski, J. G.; Kaszynski, P.; Friderichsen, A.; Abildgaard, J. Bent 2,4-Cyclopentadienylideneketene: Spectroscopic and Ab Initio Study of Reactive Intermediate. *Collect. Czech. Chem. Commun.* **1998,** *63*, 1094-1106.

26. Monnier, M.; Allouche, A.; Verlaque, P.; Aycard, J.-P. Photolysis of Matrix Isolated Cyclopropylidene Ketene: Kinetic and Theoretical Studies of the Cyclopropylidene Formation. *J. Phys. Chem.* **1995,** *99*, 5977-5985.

27. Aycard, J.-P.; Allouche, A.; Cossu, M.; Hillebrand, M. Photolysis of Matrix-Isolated Allenylketene: An Experimental and Theoretical Study of the Allenylcarbene Reactivity. *J. Phys. Chem. A* **1999,** *103*, 9013-9021.

28. Andraos, J. Bimolecular Kinetics at Low Temperatures Using FTIR Matrix Isolation Spectroscopy: Some Caveats. Thermokinetic Parameters for the Reaction of Fulvenones with Pyridine in Pyridine Matrixes. *J. Phys. Chem. A* **2000,** *104*, 1532-1543.

29. Baxter, G. J.; Brown, R. F. C.; Eastwood, F. W.; Harrington, K. J. Pyrolytic Generation of Carbonylcyclopropane (Dimethylene Ketene) and Its Dimerization to Dispiro-[2,1,2,1]-Octane-4,8-Dione. *Tetrahedron Lett.* **1975,** *16*, 4283-4284.

30. Plueg, C.; Kanaani, H.; Wentrup, C. Ketenes from N-(2-Pyridyl)Amides. *Aust. J. Chem.* **2015,** *68*, 687-692.

31. Veedu, R. N.; Kokas, O. J.; Couturier-Tamburelli, I.; Koch, R.; Aycard, J.-P.; Borget, F.; Wentrup, C. Reaction of Iminopropadienones with Amines - Formation of Zwitterionic Intermediates, Ketenes, and Ketenimines. *J. Phys. Chem. A* **2008,** *112*, 9742-9750.

32. Kaczor, A.; Gomez-Zavaglia, A.; Cardoso, A. L.; Melo, T. M. V. D. P.; Fausto, R. Methyl 3-Methyl-2h-Azirine-2-Carboxylate Photochemistry Studied by Matrix-Isolation FTIR and DFT Calculations. *J. Phys. Chem. A* **2006,** *110*, 10742-10749.

33. Mucha, M.; Mielke, Z. Structure and Photochemistry of the Methanol Complexes with Methylglyoxal and Diacetyl: FTIR Matrix Isolation and Theoretical Study. *Chem. Phys.* **2009,** *361*, 27-34.

34. Mielke, Z.; Latajka, Z.-l.; Olbert-Majkut, A.; Wieczorek, R. Matrix Infrared Spectra and Ab Initio Calculations of the Nitrous Acid Complexes with Nitrogen Monoxide. *J. Phys. Chem. A* **2000,** *104*, 3764-3769.

35. Bibas, H.; Wong, M. W.; Wentrup, C. The Vinylketene-Acylallene Rearrangement: Theory and Experiment. *Chemistry – A European Journal* **1997,** *3*, 237-248.

36. Kus, N.; Breda, S.; Reva, I.; Tasal, E.; Ogretir, C.; Fausto, R. FTIR Spectroscopic and Theoretical Study of the Photochemistry of Matrix-Isolated Coumarin. *Photochem. Photobiol.* **2007,** *83*, 1237-1253.

37. Zuhse, R. H.; Wong, M. W.; Wentrup, C. Photochemistry of Deuterated Acetylketenes: Matrix Isolation Infrared Spectroscopic and Ab Initio Studies. *J. Phys. Chem.* **1996,** *100*, 3917-3922.

38. Jackson, P.; Carter, D.; Dent, G.; Cook, B. W.; Chalmers, J. M.; Dunkin, I. R. Selective Thermolysis of the Enol Forms of Acetoacetates During Gas Chromatography, Revealed by Combined Matrix-Isolation Fourier Transform Infrared and Mass Spectrometry. *J. Chromatogr. A* **1994,** *685*, 287-293.

39. Maier, G.; Reisenauer, H. P.; Sayrac, T. Small Rings. 41. Oxirene: Intermediate or Transition State? Matrix Irradiation of Diazoketones. *Chem. Ber.* **1982,** *115*, 2192-2201.

40. Leung-Toung, R.; Wentrup, C. Direct Observation of α-Oxo Ketenes from the Photolysis of α-Diazo β-Diketones. *J. Org. Chem.* **1992,** *57*, 4850-4858.

41. Clark, R. J. H.; Foley, L. J. A Matrix Isolation Study of the Photochemically Induced Reactions of Nitrogen Dioxide with 1,2-Dibromoethene and 1,2-Dichloroethene Using Fourier Transform Infrared Spectroscopy. *Spectrochim. Acta, Part A* **2005,** *61A*, 1389-1393.

42. Clark, R. J. H.; Foley, L. J. Photochemically Induced Reactions of Ozone with 1,2-Dibromoethene and 1,2-Dichloroethene: An FT-IR Matrix Isolation Study. *J. Phys. Chem. A* **2002,** *106*, 3356-3364.

43. Davidovics, G.; Monnier, M.; Allouche, A. FT-IR Spectral Data and Ab Initio Calculations for Haloketenes. *Chem. Phys.* **1991,** *150*, 395-403.

44. Zhang, X.; Friderichsen, A. V.; Nandi, S.; Ellison, G. B.; David, D. E.; McKinnon, J. T.; Lindeman, T. G.; Dayton, D. C.; Nimlos, M. R. Intense, Hyperthermal Source of Organic Radicals for Matrix-Isolation Spectroscopy. *Rev. Sci. Instrum.* **2003,** *74*, 3077-3086.

45. Hatten, C. D.; Kaskey, K. R.; Warner, B. J.; Wright, E. M.; McCunn, L. R. Thermal Decomposition Products of Butyraldehyde. *J. Chem. Phys.* **2013,** *139*, 214303 (1-9).

46. Frisch, M. J.; Trucks, G. W.; Schlegel, H. B.; Scuseria, G. E.; Robb, M. A.; Cheeseman, J. R.; Scalmani, G.; Barone, V.; Mennucci, B.; Petersson, G. A.; Nakatsuji, H.; Caricato, M.; Li, X.; Hratchian, H. P.; Izmaylov, A. F.; Bloino, J.; Zheng, G.; Sonnenberg, J. L.; Hada, M.; Ehara, M.; Toyota, K.; Fukuda, R.; Hasegawa, J.; Ishida, M.; Nakajima, T.; Honda, Y.; Kitao, O.; Nakai, H.; Vreven, T.; J.A. Montgomery, J.; Peralta, J. E.; Ogliaro, F.; Bearpark, M.; Heyd, J. J.; Brothers, E.; Kudin, K. N.; Staroverov, V. N.; Kobayashi, R.; Normand, J.; Raghavachari, K.; Rendell, A.; Burant, J. C.; Iyengar, S. S.; Tomasi, J.; Cossi, M.; Rega, N.; Millam, J. M.; Klene, M.; Knox, J. E.; Cross, J. B.; Bakken, V.; Adamo, C.; Jaramillo, J.; Gomperts, R.; Stratmann, R. E.; Yazyev, O.; Austin, A. J.; Cammi, R.; Pomelli, C.; Ochterski, J. W.; Martin, R. L.; Morokuma, K.; Zakrzewski, V. G.; Voth, G. A.; Salvador, P.; Dannenberg, J. J.; Dapprich, S.; Daniels, A. D.; Farkas, Ö.; Foresman, J. B.; Ortiz, J. V.; Cioslowski, J.; Fox, D. J. *Gaussian 09, Revision B.01*, Gaussian, Inc.: Wallingford, CT, 2010.

47. Vasiliou, A. K.; Piech, K. M.; Reed, B.; Zhang, X.; Nimlos, M. R.; Ahmed, M.; Golan, A.; Kostko, O.; Osborn, D. L.; David, D. E.; Urness, K. N.; Daily, J. W.; Stanton, J. F.; Ellison, G. B. Thermal Decomposition of CH_3CHO Studied by Matrix Infrared Spectroscopy and Photoionization Mass Spectroscopy. *J. Chem. Phys.* **2012,** *137*, 164308(1-14).

48. Louie, M. K.; Francisco, J. S.; Verdicchio, M.; Klippenstein, S. J.; Sinha, A. Hydrolysis of Ketene Catalyzed by Formic Acid: Modification of Reaction Mechanism, Energetics, and Kinetics with Organic Acid Catalysis. *J. Phys. Chem. A* **2015,** *119*, 4347-4357.

49. Warner, B. J.; Wright, E. M.; Foreman, H. E.; Wellman, C. D.; McCunn, L. R. Products from Pyrolysis of Gas-Phase Propionaldehyde. *J. Phys. Chem. A* **2015,** *119*, 14-23.